Colloquium: Exactly solvable Richardson-Gaudin models for many-body quantum systems

J. Dukelsky*

Instituto de Estructura de la Materia, CSIC, Madrid, Spain

S. Pittel

Bartol Research Institute, University of Delaware, Newark, Delaware 19716, USA

G. Sierra

Instituto de Física Teórica, CSIC/UAM, Madrid, Spain

(Published 6 August 2004)

The use of exactly solvable Richardson-Gaudin models to describe the physics of systems with strong pair correlations is reviewed. The article begins with a brief discussion of Richardson's early work, which demonstrated the exact solvability of the pure pairing model, and then shows how that work has evolved recently into a much richer class of exactly solvable models. The Richardson solution leads naturally to an exact analogy between these quantum models and classical electrostatic problems in two dimensions. This analogy is then used to demonstrate formally how BCS theory emerges as the large-N limit of the pure pairing Hamiltonian. Several applications to problems of relevance to condensed-matter physics, nuclear physics, and the physics of confined systems are considered. Some of the interesting effects that are discussed in the context of these exactly solvable models include (i) the crossover from superconductivity to a fluctuation-dominated regime in small metallic grains; (ii) the role of the nucleon Pauli principle in suppressing the effects of high-spin bosons in interacting boson models of nuclei, and (iii) the possibility of fragmentation in confined boson systems. Interesting insight is also provided into the origin of the superconducting phase transition both in two-dimensional electronic systems and in atomic nuclei, based on the electrostatic image of the corresponding exactly solvable quantum pairing models.

CONTENTS

---

*Electronic address: dukelsky@iem.cfmac.csic.es

I. INTRODUCTION

Exactly solvable models have played a major role in helping to elucidate the physics of strongly correlated quantum systems. Examples of their extraordinary success can be found throughout the fields of condensed-matter physics and nuclear physics. In condensed matter, the most important exactly solvable models have been developed in the context of one-dimensional (1D) systems, where they can be classified into three families (Ha, 1996). The first family began with Bethe's exact solution of the Heisenberg model (Bethe, 1931). Since then a wide variety of 1D models have been solved using the Bethe ansatz. A second family consists of the so-called Tomonaga-Luttinger models (Tomonaga, 1950; Luttinger, 1963), which are solved by bosonization techniques and which have played an important role in revealing the non-Fermi-liquid properties of fermion systems in one dimension. For this reason, these systems are now called Luttinger liquids (Haldane, 1981). The third family, proposed by Calogero (1962) and Sutherland (1971) and subsequently generalized to spin systems (Haldane, 1988; Shastry, 1988), are models with long-range interactions. They have been applied to a variety of important problems, including the physics of spin systems, the quantum Hall effect, random matrix theory, electrons in one dimension, etc.

Exactly solvable models have also been developed in the field of nuclear physics, but from a different perspective. In these models, the Hamiltonian is written as a linear combination of the Casimir operators of a group decomposition chain chosen to represent the physics of a particular nuclear phase. One example is the SU(3) model of Elliott (1958a, 1958b), which describes nuclear deformation and the associated rotational motion. Others include the three dynamical symmetry limits of the U(6) interacting boson model (Iachello and Arima, 1980), which, respectively, describe rotational nuclei [the SU(3) limit], vibrational nuclei [the U(5)limit], and gamma-unstable nuclei [the O(6) limit]. These models, all exactly solvable, have been extremely useful in providing benchmarks for a description of the complicated collective phenomena that arise in nuclear systems.

Superconductivity is a phenomenon that is common to both nuclear physics and condensed-matter systems. It is typically described by assuming a pairing Hamiltonian and treating it at the level of the BCS approximation (Bardeen *et al.*, 1957), an approximation that explicitly violates particle number conservation. While this limitation of the BCS approximation has a negligible effect for macroscopic systems, it can lead to significant errors when dealing with small or ultrasmall systems. Since the fluctuations of the particle number in BCS are of the order of $\sqrt{N}$ (N being the number of particles), improvements of the BCS theory are required for systems with $N \sim 100$ particles. The number-projected BCS approximation (Dietrich *et al.*, 1964) was developed and has been used in nuclear physics for a long time. More recently it has been applied in studies of ultrasmall superconducting grains (Braun and von Delft, 1998). In the latter, it has been shown necessary to go beyond the projected BCS approximation and to resort to the exact solution (Dukelsky and Sierra, 1999) to properly describe the crossover from the superconducting regime to the pairing fluctuation regime. It was in this context that the exact numerical solution of the pairing model, published in a series of papers in the 1960s by Richardson (1963a, 1963b, 1965, 1966a, 1968) and Richardson and Sherman (1964) and independently discussed by Gaudin (1995), was rediscovered and applied successfully to small metallic grains (Sierra *et al.*, 2000). [For a review, see von Delft and Ralph (2001).] The exact Richardson solution, though present in the nuclear physics literature since the 1960s, was scarcely used until very recently, with but a few exceptions (Bang and Krumlimde, 1970; Hasegawa and Tasaki, 1987, 1993).

Soon after the initial application of the exact solution of the pairing model to ultrasmall superconducting grains, it became clear that there is an intimate connection between Richardson's solution and a different family of exactly solvable models known as the Gaudin magnet (Gaudin, 1976). The connection came through the proof of the integrability of the pairing model by Cambiaggio, Rivas, and Saraceno (1997), who identified the complete set of commuting operators of the model, the quantum invariants whose eigenvalues are the constants of motion. This made it possible to recast the pairing

Hamiltonian as a linear combination of the quantum invariants. Furthermore, by establishing a relation between the constants of motion of the pairing model and those of the Gaudin magnet, it became possible to generalize the pairing model to three classes of pairinglike models, all of which were integrable and all of which could be solved exactly for both fermion and boson systems (Amico, Di Lorenzo, and Osterloh, 2001; Dukelsky *et al.*, 2001). The potential importance of these exactly solvable models in high-T_c superconductivity and other fields of physics has recently been pointed out (Heritier, 2001). It has also recently been shown how to obtain the exact solutions of these models using the algebraic Bethe ansatz (Amico, Falci, and Fazio, 2001; von Delft and Poghossian, 2002; Zhou *et al.*, 2002; Links *et al.*, 2003), and a connection with conformal field theory and Chern-Simons theory has been established by Sierra (2000) and Asorey *et al.* (2002).

Following their initial discussion of these exactly solvable quantum models, Richardson (1977) and Gaudin (1995) proposed an exact mapping between these models and a two-dimensional classical electrostatic problem. By exploiting this analogy, they were able to derive the thermodynamic limit of the exact solution, demonstrating that it corresponds precisely to the BCS solution. Recently, the same electrostatic mapping has been used to provide a pictorial view of the transition to superconductivity in finite nuclei and to suggest an alternative geometrical characterization of this transition (Dukelsky *et al.*, 2002). Furthermore, the validity of the thermodynamic limit based on the electrostatic image has been numerically checked for very large systems (Roman *et al.*, 2002).

In this Colloquium, we review the recent progress that has been made in the use of exactly solvable pairing and pairinglike models for the description of strongly correlated quantum many-body systems. We begin with a review of the early work of Richardson and Gaudin, who first showed the exact solvability of such models. We then discuss the extension to a wider class of exactly solvable models, building on the ideas arising from their integrability. We then discuss several recent applications, to ultrasmall superconducting grains (Sierra *et al.*, 2000; Schechter *et al.*, 2001), to interacting boson models of nuclear structure (Dukelsky and Pittel, 2001), to electrons in a two-dimensional lattice (Dukelsky *et al.*, 2001), and to confined Bose systems (Dukelsky and Schuck, 2001).

II. THE MODELS OF RICHARDSON AND GAUDIN AND THEIR GENERALIZATION

A. Richardson's exact solution of the pairing model

The pairing interaction is the part of the fermion Hamiltonian responsible for the superconducting phase in metals and in nuclear matter or neutron stars. It is also responsible for the strong pairing correlations in the corresponding finite systems, namely, ultrasmall superconducting grains and atomic nuclei. Its microscopic ori-

gin, however, depends on the system under discussion. In condensed matter, it derives from the exchange of phonons between the conduction electrons. In nuclear physics, it comes about due to the short-range nature of the effective nucleon-nucleon interaction in a nuclear medium and includes contributions both from the singlet-S and triplet-P channels of the nucleon-nucleon interaction. The main feature of the pairing interaction in both cases is that it correlates pairs of particles in time-reversed states. For recent reviews, in condensed matter see Sigrist and Ueda (1991) and in nuclear physics, Dean and Hjorth-Jensen (2003).

Quite recently, the first direct sign of BCS superconductivity has been observed in a trapped degenerate gas of ^{40}K fermionic atoms. The pairing interaction in these trapped dilute systems comes from the s wave of the atom-atom interaction (Heiselberg, 2003) and is characterized by the scattering length a. This property of the pairing interaction can be experimentally controlled by imposing an external magnetic field on the system, thereby tuning the location of the associated molecular Feshbach resonance. In this way, it is possible even to change the sign of the scattering length, which is a key to producing the observed fermionic superconductivity.

We begin our discussion of Richardson's solution of the pairing model by assuming a system of N fermions moving in a set of L single-particle states l, each having a total degeneracy Ω_l, and with an additional internal quantum number m that labels the states within the l subspace. If the quantum number l represents angular momentum, the degeneracy of a single-particle level l is $\Omega_l = 2l+1$ and $-l \leq m \leq l$. In general, however, l simply labels different quantum numbers. We shall assume throughout this discussion of fermion systems that the Ω_l are even, so that for each state there is another obtained by time reversal. The operators on which the pairing Hamiltonian is based are

$$\hat{n}_l = \sum_m a^\dagger_{lm} a_{lm}, \quad A^\dagger_l = \sum_m a^\dagger_{lm} a^\dagger_{l\bar{m}} = (A_l)^\dagger, \quad (1)$$

where $a^\dagger_{lm}$ (a_{lm}) creates (annihilates) a particle in the state (lm), and the state $(l\bar{m})$ is the corresponding time-reversed state. The number operator $\hat{n}_l$, the pair creation operator $A^\dagger_l$, and the pair annihilation operator A_l close the commutation algebra:

$$[\hat{n}_l, A^\dagger_{l'}] = 2\delta_{ll'} A^\dagger_l, \quad [A_l, A^\dagger_{l'}] = 2\delta_{ll'}(\Omega_l - 2\hat{n}_l). \quad (2)$$

The corresponding algebra is SU(2).

The most general pairing Hamiltonian can be written in terms of the three operators in Eq. (1) as

$$H = \sum_l \varepsilon_l \hat{n}_l + \sum_{ll'} V_{ll'} A^\dagger_l A_{l'}. \quad (3)$$

Often a simplified Hamiltonian is considered, in which the pairing strengths $V_{ll'}$ are replaced by a single constant g, giving rise to the pairing-model or BCS Hamiltonian,

$$H_P = \sum_l \varepsilon_l \hat{n}_l + \frac{g}{2}\sum_{ll'} A^\dagger_l A_{l'}. \quad (4)$$

When g is positive, the interaction is repulsive; when it is negative, the interaction is attractive.

The approximation leading to the pairing-model Hamiltonian must be supplemented by a cutoff restricting the number of l states in the single-particle space. In condensed-matter problems this cutoff is naturally provided by the Debye frequency of the phonons. In nuclear physics, the choice of cutoff depends on the specific nucleus and on the set of active or valence orbits in which the pairing correlations develop. The cutoff in turn renormalizes the strength of the effective pairing interaction that should be used within that active space (Baldo *et al.*, 1990).

A generic state of M correlated fermion pairs and ν unpaired particles can be written as

$$|n_1, n_2, \ldots, n_L, \nu\rangle = \frac{1}{\sqrt{\mathcal{N}}}(A^\dagger_1)^{n_1}(A^\dagger_2)^{n_2} \cdots (A^\dagger_L)^{n_L}|\nu\rangle, \quad (5)$$

where $\mathcal{N}$ is a normalization constant. The number of pairs n_l in level l is constrained by the Pauli principle to be $0 \leq 2n_l + \nu_l \leq \Omega_l$, where ν_l denotes the number of unpaired particles in that level. The unpaired state $|\nu\rangle = |\nu_1, \nu_2, \ldots, \nu_L\rangle$, with $\nu = \Sigma_l \nu_l$, is defined such that

$$A_l|\nu\rangle = 0, \quad \hat{n}_l|\nu\rangle = \nu_l|\nu\rangle. \quad (6)$$

A state with ν unpaired particles is said to have *seniority* ν. The total number of collective (or Cooper) pairs is $M = \Sigma_l n_l$ and the total number of particles is $N = 2M + \nu$.

The dimension of the Hamiltonian matrix in the Hilbert space of Eq. (5) quickly exceeds the limits of large-scale diagonalization for a modest number of levels L and particles N. As an example, consider a problem involving L doubly degenerate levels and $M = N/2$ pairs. One can readily carry out full diagonalization for up to $L = 16$ and $M = 8$, for which the full dimension of the Hamiltonian matrix is 12 870. For systems with up to $L = 32$ and $M = 16$, the Lanczos method can still be used to obtain the lowest eigenvalues. But for larger values of L and M, such methods can no longer be used and it is necessary to find alternative methods to obtain physical solutions. The BCS approach is an example of an alternative approximate method. Here we focus instead on finding the exact solution, but without numerical diagonalization.

In spite of the apparent complexity of the problem, Richardson showed that the exact unnormalized eigenstates of the Hamiltonian of Eq. (4) can be written as

$$|\Psi\rangle = B^\dagger_1 B^\dagger_2 \cdots B^\dagger_M|\nu\rangle, \quad (7)$$

where the collective pair operators B_α have the form appropriate to the solution of the one-pair problem,

$$B_\alpha^\dagger = \sum_l \frac{1}{2\varepsilon_l - E_\alpha} A_l^\dagger. \tag{8}$$

In the one-pair problem, the quantities E_α that enter Eq. (8) are the eigenvalues of the pairing Hamiltonian, i.e., the *pair energies*. Richardson proposed to use the M pair energies E_α in the many-body wave function of Eq. (7) as parameters which are then chosen to fulfill the eigenvalue equation $H_P|\Psi\rangle = E|\Psi\rangle$.

We shall not repeat here the derivation of the set of equations that the pair energies must fulfill, referring the reader to Richardson and Sherman (1964). In Sec. IV, we shall return to the eigenvalue problem for more general Hamiltonians, of which the pairing Hamiltonian is a particular case.

The key conclusions from Richardson's derivation are as follows:

- The state given in Eq. (7) is an eigenstate of the pairing Hamiltonian if the M pair energies E_α satisfy the set of M nonlinear coupled equations (called the Richardson equations)

$$1 - 4g\sum_l \frac{d_l}{2\varepsilon_l - E_\alpha} + 4g\sum_{\beta(\neq\alpha)} \frac{1}{E_\alpha - E_\beta} = 0, \tag{9}$$

where $d_l = \nu_l/2 - \Omega_l/4$ is related to the effective pair degeneracy of single-particle level l

- The energy eigenvalue associated with a given solution for the pair energies is

$$E = \sum_l \varepsilon_l \nu_l + \sum_\alpha E_\alpha. \tag{10}$$

Because the Richardson method reduces the problem to solving nonlinear coupled equations, it can be used for systems well beyond the limits of either exact numerical diagonalization or the Lanczos algorithm. For example, the method can be used to obtain exact solutions for systems with $L = 1000$ and $M = 500$, for which the dimension is 2.7×10^{299}. While we cannot obtain all the solutions for such a problem, we can relatively easily obtain the lowest few for any value of the coupling constant. This means that, using the Richardson algorithm, we can study the quantum phase transition for pairing but not any phase transitions associated with temperature. To do the latter, we would need to develop the thermodynamic Bethe ansatz for application to the pairing model, as will be discussed further in the summary given in Sec. VII.

B. The Gaudin magnet

Inspired by Richardson's solution of the pairing model, and building on his previous work on the Bethe method for solving one-dimensional problems, Gaudin (1976) proposed a family of fully integrable and exactly solvable spin models. The Gaudin models are based on the SU(2) algebra of the spin operators,

$$[K^\alpha, K^\beta] = 2i\varepsilon_{\alpha\beta\gamma}K^\gamma, \tag{11}$$

where $K^\alpha = \sigma^\alpha$ ($\alpha = 1, 2, 3$) are the Pauli matrices.

A quantum model with L degrees of freedom is integrable if there exist L independent, global Hermitian operators that commute with one another. This condition guarantees the existence of a common basis of eigenstates for the L operators, called the *quantum invariants*, and for their eigenvalues, the constants of motion.

Since the SU(2) algebra has one degree of freedom, the most general set of L Hermitian operators, quadratic in the spin operators and global in L spins, are

$$H_i = \sum_{j(\neq i)=1}^{L} \sum_{\alpha=1}^{3} w_{ij}^\alpha K_i^\alpha K_j^\alpha, \tag{12}$$

where the w_{ij}^α are $3L(L-1)$ real coefficients. To define an integrable model, i.e., to satisfy the commutation relations $[H_i, H_j] = 0$, these coefficients must satisfy the system of algebraic equations

$$w_{ij}^\alpha w_{jk}^\gamma + w_{ji}^\beta w_{ik}^\gamma - w_{ik}^\alpha w_{jk}^\beta = 0. \tag{13}$$

Gaudin proposed two conditions to solve this system of equations. The first was antisymmetry of the w coefficients,

$$w_{ij}^\alpha = -w_{ji}^\alpha. \tag{14}$$

The second was to express the w coefficients as an odd function of the difference between two real parameters,

$$w_{ij}^\alpha = f_\alpha(\eta_i - \eta_j), \tag{15}$$

in order to fulfill Eq. (14).

The most general solution of Eq. (13) subject to Eqs. (14) and (15) can be written in terms of elliptic functions. We further restrict consideration here to the case in which the total spin in the z direction, $S^z = \frac{1}{2}\Sigma_i K_i^z$, is conserved, i.e., the L operators H_i (Gaudin Hamiltonians) commute with S^z. Conservation of S^z requires that $w_{ij}^x = w_{ij}^y = X_{ij}$ and $w_{ij}^z = Y_{ij}$, in terms of two new matrices X and Y. In such a case, the integrability conditions of Eq. (13) reduce to

$$Y_{ij}X_{jk} + Y_{ki}X_{jk} + X_{ki}X_{ij} = 0. \tag{16}$$

There are three classes of solutions to Eq. (16):

(I)   the rational model,

$$X_{ij} = Y_{ij} = \frac{1}{\eta_i - \eta_j}; \tag{17}$$

(II)   the trigonometric model,

$$X_{ij} = \frac{1}{\sin(\eta_i - \eta_j)}, \quad Y_{ij} = \cot(\eta_i - \eta_j); \tag{18}$$

(III)   the hyperbolic model,

$$X_{ij} = \frac{1}{\sinh(\eta_i - \eta_j)}, \quad Y_{ij} = \coth(\eta_i - \eta_j). \tag{19}$$

We shall hold off presenting details on the solutions of the three families of Gaudin models until Sec. II.D, where we discuss the generalization of the Richardson-Gaudin models. At that point we shall see that the solutions of the Gaudin models are based on precisely the same ansatz as that used by Richardson in his solution of the pairing model.

The most general integrable spin Hamiltonian that can be written as a linear combination of the Gaudin integrals of motion in Eq. (12) is

$$H = 2\sum_i \zeta_i H_i = \sum_{i \neq j} (\zeta_i - \zeta_j)\{X_{ij}[K_i^x K_j^x + K_i^y K_j^y] + Y_{ij}K_i^z K_j^z\}.$$

(20)

The above Hamiltonian, which models a spin chain with long-range interactions, has a total of $2L$ free parameters. There are L η parameters, which define the X matrices, and L ζ parameters. It can be readily confirmed that the rational family gives rise to an XXX spin model, while the trigonometric and hyperbolic families correspond to an XXZ spin model. To the best of our knowledge, there have been no physical applications of the Gaudin magnet, though there are indications that when the $2L$ free parameters of the model are chosen at random the Gaudin magnet behaves as a quantum spin glass (Arrachea and Rozenberg, 2001).

The Richardson model has a natural link to superconductivity and the Gaudin model to quantum magnetism, both very important concepts in contemporary physics. Despite these facts, neither model has received much attention from the nuclear or condensed-matter communities for many years. On the other hand, the Gaudin models have played an important role in the study of quantum integrability. For a recent reference, see Gould *et al.* (2002).

C. Integrability of the pairing model

Despite the fact that the Richardson and Gaudin models are so similar, it was not until the work of Cambiaggio, Rivas, and Saraceno (1997) that a precise connection was established. We now discuss their work and show how it provides the necessary missing link.

The key point of Cambiaggio *et al.* was to show that the pairing model is integrable by finding the set of commuting Hermitian operators in terms of which the pairing-model Hamiltonian could be expressed as a linear combination. Finding the complete set of common eigenvectors of those quantum invariant operators is then equivalent to finding the eigenvectors of the pairing-model Hamiltonian.

In their derivation, they began by introducing a pseudospin representation of the pair algebra, advancing a connection between pairing phenomena and spin physics that had been pointed out long ago by Anderson (1958).

The elementary operators of the pair algebra, defined in terms of the generators of the SU(2) pseudospin algebra, are

$$K_i^0 = \frac{1}{2}\sum_m a_{lm}^\dagger a_{lm} - \frac{1}{4}\Omega_l,$$

$$K_l^+ = \frac{1}{2}\sum_m a_{lm}^\dagger a_{l\bar{m}}^\dagger = (K_l^-)^\dagger.$$

(21)

The operator K_l^+ creates a pair of fermions in time-reversed states. The degeneracy Ω_l of level l is related to a pseudospin S_l for that level according to $\Omega_l = 2S_l + 1$. The three operators in Eq. (21) close the SU(2) commutation algebra,

$$[K_l^0, K_{l'}^\pm] = \pm\delta_{ll'}K_l^\pm, \quad [K_l^+, K_{l'}^-] = 2\delta_{ll'}K_l^0.$$

(22)

The SU(2) group for a level l has one degree of freedom and its Casimir operator is

$$(K_l^0)^2 + \frac{1}{2}(K_l^+ K_l^- + K_l^- K_l^+) = \frac{1}{4}(\Omega_l^2 - 1).$$

(23)

For a problem involving L single-particle levels, there are obviously L degrees of freedom.

Guided by previous work on the two-level pairing model, Cambiaggio *et al.* (1997) considered the following set of operators:

$$R_l = K_l^0 + 2g \sum_{l'(\neq l)} \frac{1}{\varepsilon_l - \varepsilon_{l'}}\left[\frac{1}{2}(K_l^+ K_{l'}^- + K_l^- K_{l'}^+) + K_l^0 K_{l'}^0\right].$$

(24)

They showed that these operators are (i) Hermitian, (ii) global, in the sense that they are independent of the Hilbert space, (iii) independent, in the sense that no one can be expressed as a function of the others, and (iv) commute with one another. Furthermore, there are obviously as many R_l operators as degrees of freedom. The set of L such operators thus fulfills the conditions required for the quantum invariants of a fully integrable model. Finally, they showed that the pairing-model Hamiltonian of Eq. (4) can be written as a linear combination of the R_l according to

$$H_P = 2\sum_l \varepsilon_l R_l + cte,$$

(25)

where *cte* is an uninteresting constant.

We now return to the relationship between the Richardson pairing model and the Gaudin models. This can be done by focussing on Gaudin's rational model and comparing its quantum invariants to those of Cambiaggio *et al.* [see Eq. (24)] for the pairing model. As can be readily seen, the two are very similar except that the quantum invariants of Gaudin's rational model are missing a one-body term or equivalently a linear term in the spin operators. As shown by Cambiaggio *et al.*, this term preserves the commutability of the R operators and therefore generalizes Gaudin's rational model. In the following subsection, we discuss the solution of the so-called generalized Richardson-Gaudin models that emerge when this term is added.

D. Generalized Richardson-Gaudin models

The generalization of the Richardson and Gaudin models we now discuss proceeds along two distinct lines. First, we no longer limit our discussion to Gaudin's rational model, but now generalize to all three types (rational, trigonometric, and hyberbolic). We shall see that all three can be generalized by the inclusion of a linear term in the quantum invariants. Second, we generalize our discussion to include boson models as well as fermion models.

We begin by considering the generalization to boson models. For boson systems, the elementary operators of the pair algebra are

$$K_i^0 = \frac{1}{2}\sum_m a_{lm}^\dagger a_{lm} + \frac{1}{4}\Omega_l,$$

$$K_l^+ = \frac{1}{2}\sum_m a_{lm}^\dagger a_{l\bar{m}}^\dagger = (K_l^-)^\dagger. \qquad (26)$$

Note the similarity with the fermion pair operators of Eq. (21). The only differences are that (i) there is a relative minus sign between the two terms in the operator K^0, and (ii) there is no longer a restriction to Ω_l being even. The latter point follows from the fact that for bosons a single-particle state can be its own time-reversal partner. As an example, consider scalar bosons confined to a 3D harmonic-oscillator potential, as will be discussed further in Sec. VI.D. The degeneracy associated with a shell having principal quantum number n is $\Omega_n = (n+1)(n+2)/2$. The lowest two shells ($n=0$ and 1) have odd degeneracies, whereas the next two ($n=2$ and 3) have even degeneracies.

The set of operators in Eq. (26) satisfy the commutation algebra

$$[K_l^0, K_{l'}^\pm] = \pm\delta_{ll'}K_l^\pm, \quad [K_l^+, K_{l'}^-] = -2\delta_{ll'}K_l^0, \qquad (27)$$

appropriate to SU(1,1)

In subsequent considerations, we shall often treat fermion and boson systems at the same time. To facilitate this, we can combine the relevant SU(2) commutation relations for fermions and SU(1,1) relations for bosons into the compact form

$$[K_l^0, K_{l'}^\pm] = \pm\delta_{ll'}K_l^\pm, \quad [K_l^+, K_{l'}^-] = \mp 2\delta_{ll'}K_l^0. \qquad (28)$$

When both types of systems are being treated together, we follow a convention whereby the upper sign refers to bosons and the lower sign to fermions.

Following earlier discussion, we now consider the most general Hermitian and number-conserving operator with linear and quadratic terms,

$$R_l = K_l^0 + 2g\sum_{l'(\neq l)}\left[\frac{X_{ll'}}{2}(K_l^+K_{l'}^- + K_l^-K_{l'}^+) \mp Y_{ll'}K_l^0 K_{l'}^0\right]. \qquad (29)$$

Note that this is a natural generalization of Eq. (24), but now appropriate to both boson and fermion systems.

We next look for the conditions that the matrices X and Y in Eq. (29) must satisfy in order that the R operators commute with one other. Surprisingly, the conditions are precisely those derived by Gaudin and presented in Eq. (16), despite the fact that the quantum invariants now include a linear term and that they now represent both boson and fermion systems.

Here, too, there are three families of solutions, which can be written in compact form as

$$X_{ij} = \frac{\gamma}{\sin[\gamma(\eta_i - \eta_j)]}, \quad Y_{ij} = \gamma\cot[\gamma(\eta_i - \eta_j)], \qquad (30)$$

where $\gamma\to 0$ corresponds to the rational model, $\gamma=1$ to the trigonometric model, and $\gamma=i$ to the hyperbolic model. The three limits are completely equivalent to those presented for the Gaudin magnet in Eqs. (17)–(19).

The next step is to find the exact eigenstates common to all L quantum invariants given in Eq. (29),

$$R_i|\Psi\rangle = r_i|\Psi\rangle. \qquad (31)$$

This can be accomplished by using an ansatz similar to the one used by Richardson [see Eq. (7)] to solve the pairing model, namely,

$$|\Psi\rangle = \prod_{\alpha=1}^M B_\alpha^\dagger|\nu\rangle, \quad B_\alpha^\dagger = \sum_{i=1}^L u_i(E_\alpha)K_i^+. \qquad (32)$$

The wave function in Eq. (32) is a product of collective pair operators $B_\alpha^\dagger$, which are themselves linear combinations of the raising operators K_i^+ that create pairs of particles in the various single-particle states. Note that they are analogous to the Richardson collective pair operators of Eq. (8).

We now present explicitly the solutions to the eigenvalue equations for the three models. As we shall see, it is possible to present the hyperbolic and trigonometric results in a single set of compact formulas, by using the notation sn for sin or sinh, cs for cos or cosh, and ct for cot or coth. These are not to be confused with elliptic functions. The rational model solutions are of a somewhat different structure and thus are presented separately. For each family, we first give the amplitudes u_i that define the collective pairs in terms of the free parameters η_i and the unknown pair energies E_α, then the set of generalized Richardson equations that define the pair energies E_α, and finally the eigenvalues r_i of the quantum invariants R_i.

(I) The rational model:

$$u_i(E_\alpha) = \frac{1}{2\eta_i - E_\alpha}, \qquad (33)$$

$$1 \pm 4g\sum_j \frac{d_j}{2\eta_j - E_\alpha} \mp 4g\sum_{\beta(\neq\alpha)} \frac{1}{E_\alpha - E_\beta} = 0, \qquad (34)$$

$$r_i = d_i\left[1 \mp 2g\sum_{j(\neq i)} \frac{d_j}{\eta_i - \eta_j} \mp 4g\sum_\alpha \frac{1}{2\eta_i - E_\alpha}\right]. \qquad (35)$$

(II) and (III) The trigonometric and hyperbolic models:

$$u_i(E_\alpha) = \frac{1}{\text{sn}(E_\alpha - \eta_i)}, \tag{36}$$

$$1 \mp 2g \sum_j d_j \text{ct}(E_\alpha - \eta_j) \pm 2g \sum_{\beta(\neq\alpha)} \text{ct}(E_\beta - E_\alpha) = 0, \tag{37}$$

$$r_i = d_i \left\{ 1 \mp 2g \left[\sum_{j(\neq i)} d_j \text{ct}(\eta_i - \eta_j) - \sum_\alpha \text{ct}(E_\alpha - 2\eta_i) \right] \right\}. \tag{38}$$

In Eqs. (33)–(38), the quantity d_l is now given by

$$d_l = \frac{\nu_l}{2} \pm \frac{\Omega_l}{4}. \tag{39}$$

Given a set of parameters η_i and a pairing strength g, the pair energies E_α are obtained by solving a set of M coupled nonlinear equations, either those of Eq. (34) for the rational model or those of Eq. (37) for the trigonometric or hyperbolic models. In the limit $g \to 0$, Eqs. (34) and (37) can only be satisfied for $E_\alpha \to 2\eta_i$. In this limit, the corresponding pair amplitudes $u_i(E_\alpha)$ in Eqs. (33) and (36) become diagonal and the states of Eq. (32) reduce to a product of uncorrelated pairs acting on an unpaired state. The ground state, for example, involves pairs filling the lowest possible states and no unpaired particles. Excitations involve either promoting pairs from the lowest paired states to higher ones or breaking pairs and increasing the seniority. In this way, we can follow the trajectories of the pair energies E_α that emerge from Eqs. (34) and (37) as a function of g for each state of the system.

For boson systems the pair energies are always real, whereas for fermion systems the pair energies can either be real or can arise in complex-conjugate pairs. In the latter case, there can arise singularities in the solution of Eqs. (34) and (37) for some critical value of the pairing strength g_c, when two or more pair energies acquire the same value. It was shown by Richardson (1965) that each of these critical g values is related to a single-particle level i and that at the critical point there are $1 - 2d_i$ pair energies degenerate at $2\eta_i$. These singularities of course cancel in the calculations of energies, which do not show any discontinuity in the vicinity of the critical points. However, the numerical solution of the nonlinear equations (34) and (37) may break down for values of g close to the singularities, making impractical the method of following the trajectories of the pair energies E_α from the weak-coupling limit to the desired value of the pairing strength g. Recently, Rombouts *et al.* (2003) proposed a new method based on a change of variables that avoids the singularity problem, opening the possibility of finding numerical solutions in the general case.

The eigenvalues of the R operators, given by Eqs. (35) and (38), are always real since the pair energies are either real or occur in complex-conjugate pairs. Each solution of the nonlinear set of equations produces an eigenstate common to all R_i operators, and consequently to any Hamiltonian that is written as a linear combination of them. The corresponding Hamiltonian eigenvalue is the same linear combination of r_i eigenvalues.

III. THE ELECTROSTATIC MAPPING OF THE RICHARDSON-GAUDIN MODELS; PAIRONS AND ORBITONS

We now introduce an exact mapping between the integrable Richardson-Gaudin models and a classical electrostatic problem in two dimensions. Our derivation builds on the earlier work of Richardson (1977) and Gaudin (1995), who used this electrostatic analogy to show that the exact solution of the pairing-model Hamiltonian agrees with the BCS approximation in the large-N limit. For simplicity, we concentrate here on the exact solution for the rational family ($\gamma \to 0$). The exact solution of the trigonometric and the hyperbolic families can be reduced to a set of rational equations by a proper transformation and then also interpreted as a classical two-dimensional problem (Amico *et al.*, 2002).

Let us assume that we have a two-dimensional (2D) classical system composed of a set of M free point charges and another set of L fixed point charges. For reasons that will become clear when we use these electrostatic ideas as a means of studying quantum pairing problems, we shall refer to the fixed point charges as *orbitons* and the free point charges as *pairons*.

The Coulomb potential due to the presence of a unit charge at the origin is given by the solution of the Poisson equation

$$\nabla^2 V(\mathbf{r}) = -2\pi\delta(\mathbf{r}). \tag{40}$$

The Coulomb potential $V(\mathbf{r})$ that satisfies this equation depends on the space dimensionality. For one, two, and three dimensions, respectively, the solutions are

$$V(\mathbf{r}) \sim \begin{cases} r, & \text{1D} \\ \ln(r), & \text{2D} \\ 1/r, & \text{3D}. \end{cases} \tag{41}$$

In three dimensions, the Coulomb potential has the usual $1/r$ behavior, but in two dimensions it is logarithmic. In practice, there are no 2D electrostatic systems. However, there are cases of long parallel cylindrical conductors for which the end effects can be neglected so that the problem can be effectively reduced to a 2D plane. In our case, however, we shall simply use the mathematical structure of the idealized 2D problem to obtain useful new insight into the physics of the quantum many-body pairing problem.

For the purposes of this discussion, we map the 2D xy plane into the complex plane by assigning to each point $\mathbf{r}$ a complex number $z = x + iy$. Let us now assume that the pairons have charges q_α and positions z_α, with $\alpha = 1, \ldots, M$, and that the orbitons have charges q_i and positions z_i, with $i = 1, \ldots, L$. Since they are confined to a 2D space, all charges interact with one another through a logarithmic potential. Let us also assume that there is

TABLE I. Analogy between a quantum pairing problem and the corresponding 2D classical electrostatic problem.

Quantum pairing model	Classical 2D electrostatic picture
effective single particle energy η_i	orbiton position $Z_i = 2\eta_i$
effective orbital degeneracy d_i	orbiton charge $q_i = d_i$
pair energy E_α	pairon position $z_\alpha = E_\alpha$
pairing strength g	electric-field strength $e = \pm 1/4g$

an external uniform electric field present, with strength e and pointing along the real axis. The electrostatic energy of the system is therefore

$$U = e \sum_{\alpha=1}^{M} q_\alpha \, \mathrm{Re}(z_\alpha) + e \sum_{j=1}^{L} q_j \, \mathrm{Re}(z_j)$$
$$- \sum_{j=1}^{L} \sum_{\alpha=1}^{M} q_\alpha q_j \ln|z_i - z_\alpha| - \frac{1}{2} \sum_{\alpha \neq \beta} q_\alpha q_\beta \ln|z_\alpha - z_\beta|$$
$$- \frac{1}{2} \sum_{i \neq j} q_i q_j \ln|z_i - z_j|. \qquad (42)$$

If we now look for the equilibrium position of the free pairons in the presence of the fixed orbitons, we obtain the extremum condition

$$e + \sum_{j} \frac{q_j}{z_j - z_\alpha} - \sum_{\beta(\neq\alpha)} \frac{q_\beta}{z_\alpha - z_\beta} = 0. \qquad (43)$$

It can be readily seen that the Richardson equations for the rational family (34) coincide with the equations for the equilibrium position of the pairons (43), *if* the pairon charges are $q_\alpha = 1$, the pairon positions are $z_\alpha = E_\alpha$, the orbiton charges q_i are equal to the effective level degeneracies d_i (which for the ground configuration are $\pm \Omega_i/4$), the orbiton positions are $z_i = 2\eta_i$, and the electric field strength is $e = \pm 1/4g$.

As a reminder, the η_i's are free parameters defining the integrals of motion from which the generalized Richardson-Gaudin Hamiltonian is derived [see Eq. (15)]. In the case of the pure pairing-model Hamiltonian, which is a specific Hamiltonian in the rational family, they are the single-particle energies of the active levels. In any subsequent discussion in which they are used, we shall thus refer to them as effective single-particle energies.

Table I summarizes the relationship between the quantum pairing model and the classical electrostatic problem implied by the above analogy.

From the above discussion, we see that solving the Richardson equations for the pair energies E_α is completely equivalent to finding the stationary solutions for the pairon positions in the analogous classical 2D electrostatic problem.

Assuming that the real axis is vertical and the imaginary axis horizontal, and taking into account that the orbiton positions are given by the real single-particle energies, it is clear that they must lie on the vertical axis.

The pairon positions are not of necessity constrained to the vertical axis, but rather must be reflection symmetric around it. This reflection symmetry property can be readily seen by performing complex conjugation on the electrostatic energy functional (42). As a consequence, a pairon must either lie on the vertical axis (for real pair energies) or must be part of a mirror pair (for complex pair energies).

The various stationary pairon configurations can be readily traced back to the weakly interacting system ($g \rightarrow 0$). In this limit, the pairons for a fermionic system are distributed around (and very near to) the orbitons, thereby forming compact artificial *atoms*. The number of pairons surrounding orbiton i cannot exceed $|2d_i|$, as required by the Pauli principle, i.e., we cannot accommodate in a single level more particles than its degeneracy permits. The lowest-energy (ground-state) configuration corresponds to distributing the pairons around the lowest-position orbitons consistent with the Pauli constraint. We then let the system evolve gradually with increasing g until we reach its physical value. Of course, the Pauli limitation does not apply to boson systems, examples of which are discussed in Sec. VI.

To illustrate how the analogy applies for a specific quantum pairing problem involving fermions, we consider the atomic nucleus ^{114}Sn. This is a semimagic nucleus, which can be modeled as 14 valence neutrons occupying the single-particle orbits of the $N = 50-82$ shell. Furthermore, it can be meaningfully treated in terms of a pure pairing-model Hamiltonian with single-particle energies extracted from experiment. We shall return to this problem briefly in Sec. VI.B. For now we simply want to use this problem to illustrate the relationship between the quantum parameters and the electrostatic parameters for the analogous classical problem.

In Table II, we list the relevant single-particle orbits of the 50–82 shell in the third column, their corresponding single-particle energies in the first column, and the associated degeneracies in the second. Each level corresponds to an orbiton in the electrostatic problem, with the position of the orbiton given in the fourth column (at twice the single-particle energy of the corresponding single-particle level). Note that this is always purely real, meaning that in the 2D plot each orbiton has $y = 0$. Finally, in the fifth column we give the charge of the orbiton, which is simply related to the degeneracy of the level according to the prescription in Table I.

To illustrate the weak-pairing limit discussed above,

TABLE II. Relationship between the quantum pairing problem for the nucleus ^{114}Sn and the corresponding 2D classical problem. The single-particle energies are in MeV.

Single-particle energy	Single-particle degeneracy	Single-particle level/orbiton	Orbiton position	Orbiton charge
0.0	6	$d_{5/2}$	0.0	−1.5
0.22	8	$g_{7/2}$	0.44	−2.0
1.90	2	$s_{1/2}$	3.80	−0.5
2.20	4	$d_{3/2}$	4.40	−1.0
2.80	12	$h_{11/2}$	5.60	−3.0

we show in Fig. 1 the pairon positions associated with the electrostatic solution for ^{114}Sn calculated for a pairing strength of $g=-0.02$ MeV, well below the strength at which the superconducting phase transition sets in. Solid lines connect each pairon to its nearest neighbor. As we can readily see, the seven pairons in this case indeed distribute themselves very near to the lowest two orbitons, with three forming an artificial atom around the $d_{5/2}$ and four forming an artificial atom around the $g_{7/2}$.

IV. THE LARGE-*N* LIMIT

We now discuss how the electrostatic mapping of the previous section can be used to study the exact solution of the pairing problem in the large-N or thermodynamic limit. We focus on fermion systems and consider the pairing-model (or BCS) Hamiltonian used by von Delft *et al.* (1996) to describe the physics of ultrasmall superconducting grains,

$$H_{BCS} = \frac{1}{2}\sum_{j\sigma=\pm} \epsilon_j a_{j\sigma}^\dagger a_{j\sigma} - G\sum_{jj'} a_{j+}^\dagger a_{j-}^\dagger a_{j'-} a_{j'+}, \quad (44)$$

where $a_{j\pm}$ and $a_{j\pm}^\dagger$ are annihilation and creation operators, respectively, in the time-reversed single-particle states $|j\pm\rangle$, both with energies $\varepsilon_j = \epsilon_j/2$, and G is the BCS dimensionful coupling constant. Thus ϵ_j denotes the energy of a pair occupying the level j and $\epsilon_i \neq \epsilon_j$ for $i \neq j$.

This model was solved analytically by Richardson and Sherman (1964) and numerically up to $L=32$ single-particle levels by Richardson (1966a). The seniority-zero eigenstates for a system of M fermions depend on a set of parameters E_ν $(\nu=1,\ldots,M)$ (the pair energies) that are, in general, complex solutions of the M coupled algebraic Richardson equations,

$$\frac{1}{G} = \sum_{j=1}^{L} \frac{1}{\epsilon_j - E_\nu} - \sum_{\mu=1(\neq\nu)}^{M} \frac{2}{E_\mu - E_\nu}, \quad \nu=1,\ldots,M.$$

$$(45)$$

The energy E associated with a given solution is given by the sum of the resulting pair energies [see Eq. (10)]. The ground state is given by the solution of Eq. (45) with the lowest value of E.

In Fig. 2, we plot the solution of Eq. (45) for a model of equally spaced energy levels, $\epsilon_j = d(2j-L-1)$,

FIG. 1. Two-dimensional representation of the pairon positions in ^{114}Sn for a pure pairing-model Hamiltonian with single-particle energies as given in Table II and with $g=-0.02$ MeV.
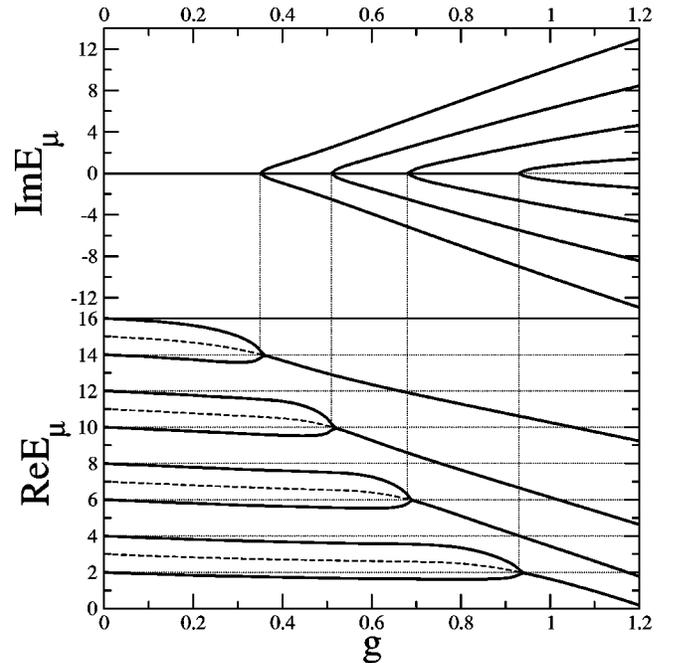
FIG. 2. Evolution of the real and imaginary parts of $E_\mu(g)$, in units of $d=\omega/L$, for the equally spaced model with $M=L/2=8$, as a function of the coupling constant g. For convenience, the energy levels are chosen in this figure as $\epsilon_j=2j$. From Roman *et al.*, 2002.
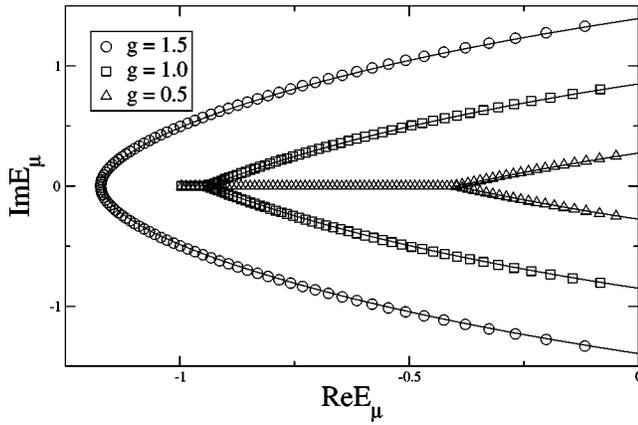
FIG. 3. Plot of the roots E_μ for the equally spaced pairing model in the complex ξ plane. The discrete symbols denote the numerical values for $M=100$. All energies are in units of ω. From Roman *et al.*, 2002.

$j=1,\dots,L$, where $d=\omega/L$ is the single-particle level spacing and ω is twice the Debye energy. The calculation is done at half filling for $M=L/2=8$. Note: At half filling, the number of levels L is equal to the number of particles N. For small values of the coupling constant $g=GL$ all the solutions E_μ are real, but as we approach some critical value $g_{c,1}$ the two roots closest to the Fermi level develop into a complex-conjugate pair. The same phenomenon happens to other roots as g is further increased, until eventually all of the roots form complex pairs. This fact was observed by Richardson (1977) and Gaudin (1995) and suggested a way to analyze systems with a large number of particles, where the exact solution must converge asymptotically to the BCS solution.

Figure 3 shows the solutions to Eq. (45) for a system with a much larger number of particles, $M=N/2=100$ pairs, and for three values of g. For $g=1.5$, the roots E_μ form an arc which ends at the points $2\lambda \pm 2i\Delta$, where λ is the BCS chemical potential and Δ the BCS gap. For $g=1.0$ and 0.5, the set of roots consist of two pieces, one formed by an arc Γ with endpoints $2\lambda \pm 2i\Delta$ which touches the real axis at some point ε_A, and a set of real roots along the segment $[-\omega, \varepsilon_A]$. As g decreases, the latter segment gets progressively larger while the arc becomes smaller and eventually shrinks to a point when $g=0$.

The solid lines in the figure are the results obtained from the algebraic equations derived by Gaudin (1995) in the large-N limit. Note that they are in excellent agreement with the results obtained by numerically solving Eq. (45).

We now show how to make the connection between the large-N limit of the pairing-model problem and BCS theory more precise, by applying the electrostatic analogy introduced in Sec. III. We shall consider the limit in which $L \to \infty$, while keeping fixed the following quantities:

$$G = \frac{g}{L}, \quad \rho = \frac{M}{L}. \tag{46}$$

Assuming that the pair energies organize themselves into an arc Γ which is piecewise differentiable and symmetric under reflection on the real axis, Eq. (45) (the Richardson equation) in the continuum limit is converted into the integral equation

$$\int_\Omega \frac{\rho(\epsilon)d\epsilon}{\epsilon - \xi} - P\int_\Gamma \frac{r(\xi')|d\xi'|}{\xi' - \xi} - \frac{1}{2G} = 0, \quad \xi \in \Gamma, \tag{47}$$

where $\rho(\epsilon)$ is the energy density associated with the energy levels that lie in the interval $\Omega = [-\omega, \omega]$ and satisfies

$$\int_\Omega \rho(\epsilon)d\epsilon = \frac{L}{2}, \tag{48}$$

while $r(\xi)$ is the density of the roots E_μ that lie in the arc Γ and satisfies

$$\int_\Gamma r(\xi)|d\xi| = M, \tag{49}$$

$$\int_\Gamma \xi r(\xi)|d\xi| = E. \tag{50}$$

The last equation is a consequence of Eq. (10). The solution of Eq. (47) was given by Gaudin (1995) using techniques of complex analysis. We now summarize his main results, which from a different perspective were also given by Richardson (1977). A detailed derivation of the continuum limit together with a comparison with numerical results for large but finite systems was presented by Roman *et al.* (2002).

Introducing an "electric field," and studying its properties in the vicinity of the arc Γ, one can show that Eq. (47) yields the well-known BCS gap equation

$$\int_\Omega \frac{\rho(\epsilon)d\epsilon}{\sqrt{\left(\frac{\epsilon}{2} - \lambda\right)^2 + \Delta^2}} = \frac{1}{G}, \tag{51}$$

that Eq. (49) becomes the equation for the chemical potential

$$M = \int_\Omega \left(1 - \frac{\frac{\epsilon}{2} - \lambda}{\sqrt{\left(\frac{\epsilon}{2} - \lambda\right)^2 + \Delta^2}}\right)\rho(\epsilon)d\epsilon, \tag{52}$$

and that Eq. (50) gives the BCS expression for the ground-state energy,

$$E = -\frac{\Delta^2}{G} + \int_\Omega \left(1 - \frac{\frac{\epsilon}{2} - \lambda}{\sqrt{\left(\frac{\epsilon}{2} - \lambda\right)^2 + \Delta^2}}\right)\rho(\epsilon)\epsilon d\epsilon. \tag{53}$$

Thus by using the electrostatic analogy for the quantum pairing problem we are able to demonstrate how the BCS equations emerge naturally in the large-N limit.

V. THE ELEMENTARY EXCITATIONS OF THE BCS HAMILTONIAN

Most of the studies to date of excited states of the BCS Hamiltonian [see Eq. (44)] based on Richardson's exact solution have dealt with a subclass of these states, namely, those obtained by breaking a single Cooper pair. In a case involving doubly degenerate levels only, the levels in which the broken pair reside can no longer be occupied by the collective pairs. Those levels are thus *blocked* and this is reflected in the Richardson equations by their having an effective degeneracy $d_l=0$. For more general pairing problems, with degeneracies larger than 2, a broken pair will not completely block a single-particle level, but rather will increase the seniority ν_l of the level and give rise to a reduced effective degeneracy $d_i=\nu_i/2-\Omega_i/4$. There is also another class of collective excitations that arises without changing the seniority. These excitations, known in nuclear physics as *pairing vibrations*, correspond to the different solutions of the Richardson equations for a given seniority configuration ν_i.

In a mean-field treatment of the same Hamiltonian, the lowest such excitations of both types correspond to two quasiparticle states in the BCS approximation, which are then mixed by the residual interaction in the random phase approximation (RPA). While this bears no obvious resemblance to the Richardson approach for these elementary excitations, it is clear that they should coincide in the large-N limit.

To investigate this relation, we focus, for simplicity, on the BCS Hamiltonian of Eq. (44) and study systematically its excited states for systems with a fixed number of particles. Once we know the excited states, we can try to interpret them in terms of elementary excitations characterized by definite quantum numbers, statistics, and dispersion relations. A generic excited state will then be given by a collection of elementary excitations.

The elementary excitations within the exact Richardson approach are associated with the number of pair energies N_G, either real or in complex-conjugate pairs, that in the large-g limit stay finite, trapped between single-particle energy levels (Roman *et al.*, 2003; Yuzbashyan *et al.*, 2003). We display this behavior in Fig. 4 for the ground state ($N_G=0$) and the first two excited states, with $N_G=1,2$, respectively, for a system with $L=40$ single-particle levels at half filling ($M=20$) as a function of g.

In the large-g limit, the pair energies that stay finite (E_ν^f) satisfy the Gaudin equation

$$\sum_{j=1}^{L} \frac{1}{\epsilon_j-E_\nu^f} - \sum_{\mu=1(\neq\nu)}^{N_G} \frac{2}{E_\mu^f-E_\nu^f} = 0, \quad \nu=1,\ldots,N_G,$$

(54)

while the remaining $M-N_G$ pair energies (E_ν^i) go to infinity and are the solution of the generalized Stieltjes problem encountered by Shastry and Dhar (2001) in the
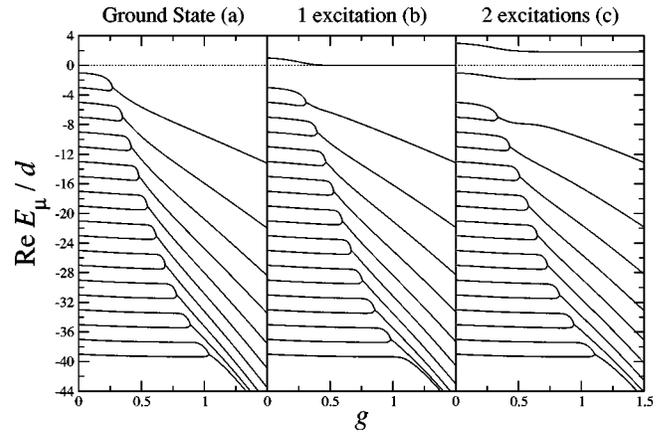
FIG. 4. Real part of E_μ for the equally spaced pairing model with $M=L/2=20$ pairs and $N_G=0, 1, 2$ excitations. From Roman *et al.*, 2003.

study of the excitations of the ferromagnetic Heisenberg model,

$$\frac{1}{g} + \frac{L}{E_\nu^i} + \sum_{\mu=1(\neq\nu)}^{M-N_G} \frac{2}{E_\mu^i-E_\nu^i} = 0, \quad \nu=1,\ldots,M-N_G.$$

(55)

The fact that the elementary excitations are related to the trapped pair energies can be readily seen in Fig. 5, where we show the low-lying excited states for the same system as in Fig. 4. We see a clear transition from the normal system at small g, where the states are classified by the single-particle configurations, to a superconducting system for $g\sim 0.3$. That the crossings take place around the transition region is a unique characteristic of an integrable model. Observation of level repulsion in the spectrum would immediately signal nonintegrability.

In the extreme superconducting limit ($g\to\infty$), the states with the same number N_G of excitations are de-
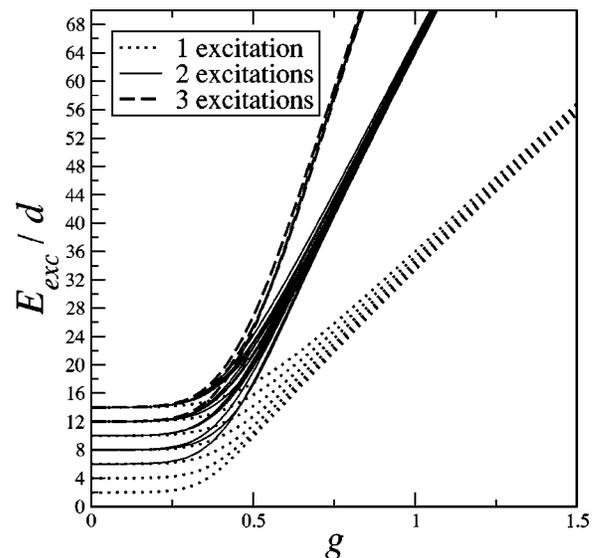
FIG. 5. Lowest 44 excitation energies $E_{exc}=E-E_{GS}$ for $M=20$ pairs at half filling. From Roman *et al.*, 2003.
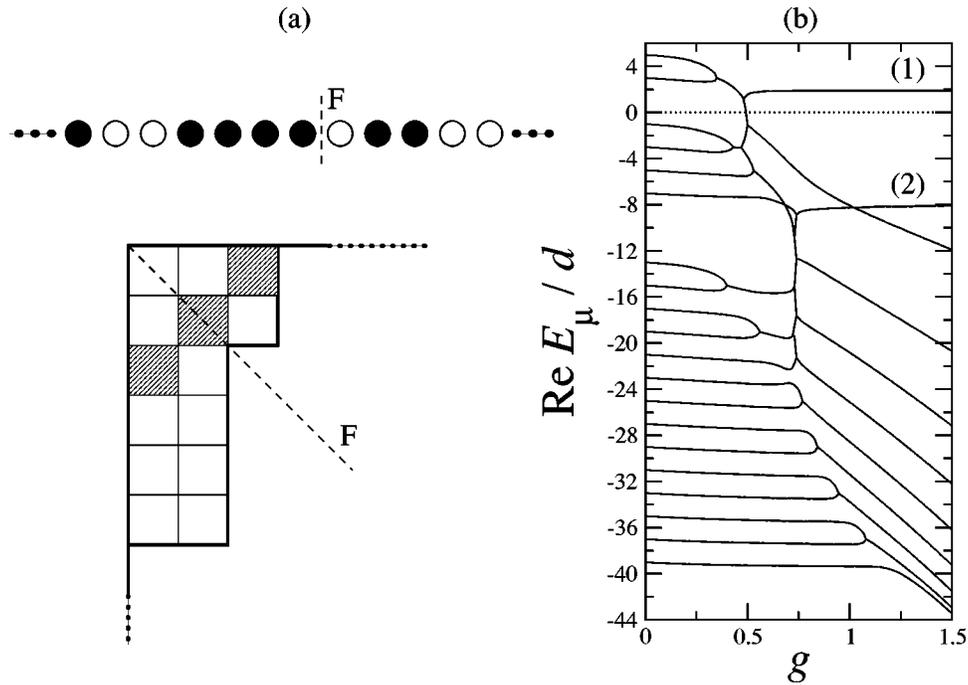
FIG. 6. An illustration of the algorithm for determining the number of roots N_G, for a case with $N_G=3$: (a) Top, initial state at $g=0$, where each solid circle (●) denotes a level occupied by a pair, each empty circle (○) denotes an empty level, and the vertical dashed line with an F near it denotes the position of the Fermi surface; bottom, the associated Young diagram; (b) real part of E_μ. From Roman *et al.*, 2003.

generate. Moreover, the slope of the excitation energies in that limit is given by N_G.

The degeneracies of the states in the extreme superconducting limit d_{L,M,N_G} have been obtained by Gaudin using the fact that the Richardson model maps onto the Gaudin magnet in this limit, and are given by

$$d_{L,M,N_G} = C_{N_G}^L - C_{N_G-1}^L, \quad 0 \le N_G \le M, \qquad (56)$$

where C_N^L is the combinatorial number of N permutations of L numbers. They satisfy the sum rule $C_M^L = \Sigma_{N_G=0}^M d_{L,M,N_G}$, so that the sum of degeneracies is the total degeneracy.

In general, the practical way to solve the Richardson equations is to start with a given configuration at $g=0$ and to let the system evolve with increasing g. Hence the problem is to find for each initial state the number of roots N_G that remain finite in the $g\to\infty$ limit. This is a highly nontrivial problem as it connects the two extreme cases of $g=0$ and $g=\infty$. The algorithm that relates each unperturbed configuration to N_G has been worked out by Roman *et al.* (2003) in terms of Young diagrams. We shall not give further details here, but show in Fig. 6 a particular example with $N_G=3$ to illustrate the complexity of the evolution of the real part of the pair energies as a function of g. For sufficiently large values of g and after a complicated pattern of fusion and splitting of roots (2 real roots↔1 complex root), the final result of $N_G=3$ emerges.

These results show the nontrivial nature of the elementary excitations of the pairing model, as exempli-

fied by their nontrivial counting. As noted above, the elementary excitations satisfy an effective Gaudin equation. They also satisfy a dispersion relation similar to that of Bogolioubov quasiparticles. For these reasons, this new type of elementary excitation has been called *gaudinos* by Roman *et al.* (2003). An interesting problem, which has been partially addressed by Yuzbashyan *et al.* (2003), would be to analyze in detail the relation between gaudinos and Bogolioubov quasiparticles for large systems.

VI. APPLICATIONS

A. Ultrasmall superconducting grains

Anderson (1959) made the conjecture that superconductivity must disappear for metallic grains when the mean level spacing d, which is inversely proportional to the volume, is of the order of the superconducting gap in bulk, Δ. A simple argument supporting this conjecture is that the ratio Δ/d measures the number of electronic levels involved in the formation of Cooper pairs, so that when $\Delta/d \le 1$ there are no active levels accessible to build pair correlations. Apart from some theoretical studies, this conjecture remained largely unexplored until the recent fabrication of ultrasmall metallic grains.

Ralph, Black, and Tinkham (1997), in a series of experiments, studied the superconducting properties of ultrasmall aluminum grains at the nanoscale. These grains have radii ~4–5 nm, mean level spacings $d\sim0.45$ MeV, Debye energies $\omega_D\sim34$ MeV, and charging energies

$E_C \sim 46$ MeV. Since the bulk gap of Al is $\Delta \sim 0.38$ MeV, this satisfies Anderson's condition, $d \geq \Delta$, for the possible disappearance of superconductivity. Moreover, the large charging energy E_C implies that these grains have a fixed number of electrons, while the Debye frequency gives an estimate of the number of energy levels involved in pairing, namely, $\Omega = 2\omega_D / d \sim 150$, which is rather small. Among other things, Ralph *et al.* (1997) found an interesting parity effect, similar to what is known to occur in atomic nuclei, whereby grains with an even number of electrons display properties associated with a superconducting gap, while the odd grains show gapless behavior.

These experimental findings produced a burst of theoretical activity focused on the study of the pairing Hamiltonian [Eq. (44)] with equally spaced levels, i.e., $\varepsilon_j = jd$. Many different approaches were used to study this model including (i) BCS approximation projected on parity (von Delft *et al.*, 1996); (ii) number-conserving BCS approximation (Braun and von Delft, 1998); (iii) Lanzcos diagonalization with up to $\Omega = 23$ energy levels (Mastellone *et al.*, 1998); (iv) perturbative renormalization group combined with small diagonalization (Berger and Halperin, 1998); (v) the density-matrix renormalization group (DMRG) with up to $\Omega = 400$ levels (Dukelsky and Sierra, 1999), etc. [For a review on this topic, see von Delft and Ralph (2001).] Following this flurry of work, it was suddenly realized that the pairing model under investigation had in fact been solved exactly in the manner of Bethe by Richardson long before. This came as a surprise and led to *a posteriori* confirmation of the results obtained by the "exact" numerical methods, namely, Lanzcos diagonalization and the DMRG. Moreover, the rediscovery of the Richardson solution produced other important new developments, including generalization of its solution, new insight from the point of view of integrable vertex models, connection with conformal field theory, Chern-Simons theory, etc. [For a review, see Sierra (2002).]

Returning to the application of the Richardson solution to ultrasmall superconducting grains, we shall focus on two quantities, the condensation energy and the Matveev-Larkin parameter (Matveev and Larkin, 1997). The condensation energy is the difference between the ground-state energy of the pairing Hamiltonian and the energy of the Fermi state (FS), namely, the Slater determinant obtained by simply filling all levels up to the Fermi surface. It is given by

$$E_b^C = E_b^{GS} - \langle FS | H_{BCS} | FS \rangle, \tag{57}$$

where $b = 0$ for even-parity grains and $b = 1$ for those with odd parity. In the BCS solution, appropriate when the number of electrons N is very large, the leading-order behavior of E_b^C is given by $-\tilde{\Delta}^2 / (2d)$, where $\tilde{\Delta}$ is the BCS gap in bulk and d scales as $1/N$, suggesting that E_b^C is independent of the parity b of the system. However, an odd ultrasmall grain has a single electron occupying the level nearest to the Fermi energy. One can easily show that this electron decouples from the dy-

namics of the pairing Hamiltonian, since the pairing interaction only scatters pairs from energy levels that are doubly occupied to those that are empty. Hence the single electron only contributes through its free energy. Furthermore, since there is one less active level at the Fermi energy, it is harder for the pairing interaction to overcome the gap, and the total energy thus increases. This is the physical origin of the parity effect in superconducting grains.

Recall that the BCS gap in bulk is given by $\tilde{\Delta} = dN/\sinh(1/g)$, with $g = 0.224$ for aluminum grains. The BCS result is obtained by solving the gap equation with a finite number of energy levels N. For even grains, there is a critical value of the ratio $d_0^c / \tilde{\Delta} = 3.53$, above which there is no solution to the gap equation. If the grains are odd, the singly occupied ("blocked") level must be eliminated from the Hamiltonian, and the critical ratio becomes $d_1^c / \tilde{\Delta} = 0.89$. The fact that this is smaller than the even critical ratio indicates that odd grains are less superconducting than even grains. Thus BCS provides an explanation of the parity effect observed by Ralph *et al.* (1997). At the same time, it suggests the existence of an abrupt crossover between the superconducting regime and the normal state, as conjectured originally by Anderson.

However, the BCS ansatz does not have a definite number of particles, which it only fixes on average. Though irrelevant for a macroscopic sample, this can be important for systems with a small number of particles, in which fluctuations in the phase of the superconducting order parameter may destroy the superconductivity. For this reason, Braun and von Delft (1998) considered the number-conserving BCS state, which includes number projection and thus does not suffer from this limitation. There are several important differences between the results obtained with number projection and without. First, the condensation energies E_b^C from the number-projection BCS ansatz are much lower than those from a corresponding BCS treatment. Second, the sharp transition between the superconducting regime and the fluctuation-dominated regime that arises in BCS is smoothed out by number-projection BCS. Nevertheless, some BCS features survive the inclusion of number projection, particularly for odd grains. Lastly, in contrast to BCS, there is always a solution to the number-projection BCS equations.

In the upper panel of Fig. 7, we compare the results of the condensation energy for even and odd grains as a function of the grain size calculated in the number-projection BCS approximation and exactly. The number-projection results show an abrupt change at the critical level spacing values $d_0^C \approx 0.5\tilde{\Delta}$ for the even systems and $d_0^C \approx 0.25\tilde{\Delta}$ for the odd systems, thereby signaling a breakdown of the superconductivity. The critical value of the mean level spacing separates two well-defined regimes, the fluctuation-dominated regime characterized by an intensive behavior of the condensation energy (E^C almost independent of d) and the extensive supercon-
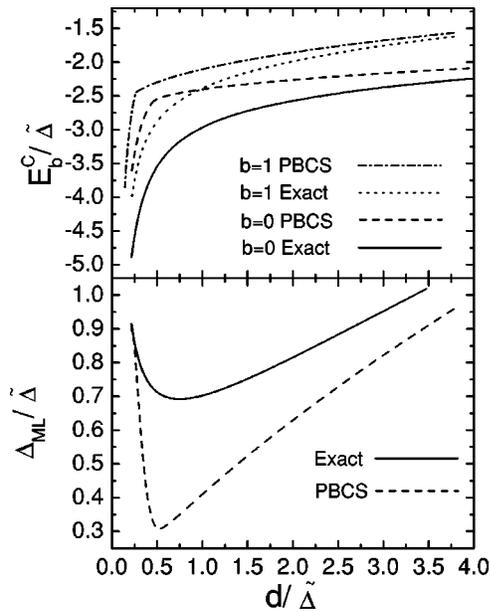
FIG. 7. Calculated results for ultrasmall superconducting grains as a function of the grain size. The upper panel gives the condensation energies E_b^C for even ($b=0$) and odd ($b=1$) grains calculated using the number-projected BCS and exact wave functions. The lower panel gives the Matveev-Larkin gap, Δ_{ML}, obtained in number-projected BCS calculations (Braun and von Delft, 1998) and in exact calculations.

ducting regime where it can be shown that the condensation energy is proportional to the volume ($E^C \sim 1/d$). The exact solution shows a completely smooth transition between superconducting and fluctuation dominated, although one can still talk about two asymptotic regimes that match near the level spacing for which the Anderson criterion $d/\tilde{\Delta} \sim 1$ is satisfied.

Another characterization of the parity effect is in terms of the gap parameter, which measures the difference between the ground-state energy of an odd grain and the mean energy of the neighboring even grains obtained by adding and removing one electron,

$$\Delta_{ML} = E_1(N) - \frac{1}{2}[E_0(N+1) + E_0(N-1)]. \qquad (58)$$

The lower panel in Fig. 7 compares the value of $\Delta_{ML}/\tilde{\Delta}$ computed at the level of the number-projection BCS approximation and exactly. Both curves show a minimum in this quantity as a function of $d/\tilde{\Delta}$. This latter feature was first conjectured by Matveev and Larkin (1997), which is why the associated gap is called the *Matveev-Larkin parameter*. It was subsequently confirmed by Mastellone *et al.* (1998) using the Lanczos method, by Berger and Halperin (1998) using the perturbative renormalization group combined with small diagonalization, by Braun and von Delft (1998) using the number-projection BCS method, and by Dukelsky and Sierra (2000) using the DMRG method. The shape of the exact curve, which is identical to that obtained using the DMRG, is rather smooth as compared with the
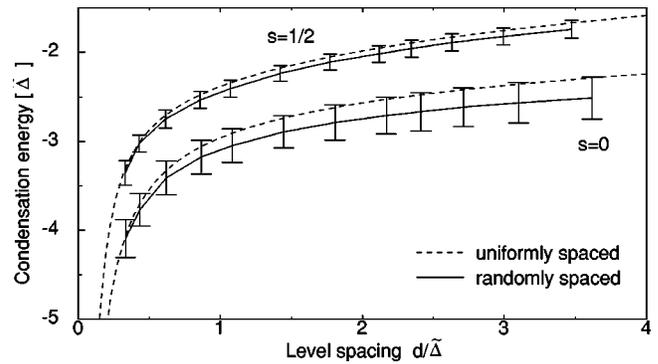
FIG. 8. Exact even and odd condensation energies E_b^C for uniform equally spaced levels (dashed line), and the ensemble-averaged energies $\langle E_b^C \rangle$ for randomly-spaced levels (solid line). The height of the fluctuation bars gives the variances δE_b^C. From Sierra *et al.*, 2000.

number-projection BCS method. This can be interpreted as a suppression of the even-odd parity effect.

Richardson's exact solution of the pairing model can also be used to study the interplay of randomness and interactions in a nontrivial model, by examining the effect of level statistics on the superconducting/fluctuation-dominated crossover, as reflected for example in the location of the critical level spacing. There was an earlier study of the latter question by Smith and Ambegaokar (1996) using the BCS approach; they concluded that randomness enhances pairing correlations. More specifically, they compared the results for a pairing model with a random spacing of levels (distributed according to a Gaussian orthogonal ensemble) with one having uniform spacings. What they showed is that for both models the BCS theory gives rise to an abrupt superconducting/fluctuation-dominated crossover, that the random-spacing Hamiltonian produces a lower correlation energy E_b^C than the corresponding uniform-spacing model, and that the average value of the critical level spacing in the model based on random splittings is larger than the corresponding value for the uniform-spacing model. As noted earlier, however, the mean-field BCS theory produces an abrupt vanishing of E_b^C that is not present in more sophisticated treatments. This raises the question of whether the conclusions they found regarding the role of randomness may be an artifact of the BCS approach.

Indeed, the exact results shown in Fig. 8 for random levels show that the superconducting/fluctuation-dominated crossover is as smooth as for the case of uniformly spaced levels. This means, remarkably, that even in the presence of randomness, pairing correlations never vanish, no matter how large $d/\tilde{\Delta}$ becomes. Quite the contrary, the randomness-induced lowering of E^C is found to be strongest in the fluctuation-dominated regime.

B. A pictorial representation of pairing in a two-dimensional lattice

We next apply the electrostatic analogy to a model of electrons in a two-dimensional lattice with a residual

TABLE III. Positions and charges of the orbitons for an attractive 2D pairing model.

$2\epsilon_k$	-8	-6	-4	-2	0	2	4	6	8
$-\Omega_k/4$	$-1/2$	-2	-2	-2	-5	-2	-2	-2	$-1/2$

pairing interaction (Dukelsky *et al.*, 2001). Assuming a nearest-neighbor hopping term, the single-electron energies in momentum space are $\varepsilon_k = -2(\cos k_x + \cos k_y)$, with $k_\sigma = 2\pi n_\sigma/P$ and $-P/2 \leq n_\sigma < P/2$. In this expression, $\sigma = x, y$ and P is the number of sites on each side of the square lattice. In the numerical example that follows, we consider a 6×6 square lattice at half filling ($M = 18$) with a constant and attractive pairing Hamiltonian for which $\varepsilon_k = \eta_k$. Table III shows the corresponding information on the positions and charges of the orbitons in the subspace of seniority-zero states.

Figure 9 shows the equilibrium positions of the pairons associated with the ground-state solution for three values of g. The orbitons are represented by open circles with radii proportional to the charges, and the pairons are represented by solid circles. For each pairon in the figure, we draw a line connecting it to the one that is closest to it.

In the limit of weak pairing ($g = -0.040$), five pairons surround the half filled orbiton with charge -5 located at the Fermi energy. The other 13 pairons are distributed close to the lowest orbitons, consistent with the Pauli principle. As is clear from the figure, for weak pairing the pairons organize themselves as artificial atoms around their corresponding orbitons. As g increases, the pairons repel, causing the atoms to expand. For $g = -0.064$ the two orbitons closest to the Fermi energy have already lost their pairons, which are forming a

pairon cluster with those from the next closest orbiton, while the remaining five pairons are still attached to their orbitons. We claim that this delocalization effect in the classical problem is a reflection of the transition from a normal system (independent atoms) to a superconducting system (collective cluster) in the quantum problem. By $g = -0.130$, the cluster has grown to the point that all pairons are trapped in it. This is the extreme superconducting limit, in which all electron pairs are participating in the superconductive phenomenon.

Similar results have been reported by Dukelsky *et al.* (2002) for the problem of pairing between like nucleons in atomic nuclei. The analysis was for two isotopes of Sn, including the isotope [114]Sn briefly alluded to in Sec. II. There, too, the superconducting phase transition was seen to be associated with a transition from isolated atoms to a cluster in the analogous electrostatic picture. Furthermore, there, too, the transition to full superconductivity was seen to develop in steps, depending on the single-particle levels that played a role in producing the pair correlations and their energy hierarchy.

The analysis of pairing in nuclei reported by Dukelsky *et al.* (2002) assumed a pure pairing-model interaction. Of course, this is just an approximation to the true nuclear interaction in the $J^\pi = 0^+$ channel. Nevertheless, we expect that the general features of the transition to superconductivity should be the same even for a more realistic pairing interaction. It is in fact possible to build greater flexibility into the nuclear structure analysis, while still preserving the electrostatic analogy, by considering more general exactly solvable Hamiltonians of the rational family.

FIG. 9. Two-dimensional representation of the positions of the orbitons and pairons corresponding to a 6×6 lattice at half filling, for three selected values of g. The orbitons are represented by open circles and the pairons by solid circles, with radii proportional to their charges.

C. Electrostatic image of interacting boson models

As an example of the use of the electrostatic mapping for a finite boson system, we now discuss the phenomenological interacting boson model of nuclei (Iachello and Arima, 1980). This model captures the collective dynamics of nuclear systems by representing correlated pairs of nucleons with angular momentum L by ideal bosons with the same angular momentum. In its simplest version, known as IBM1, there is no distinction between protons and neutrons, and only angular momentum $L = 0$ (s) and $L = 2$ (d) bosons are retained. We shall use the electrostatic image to study the properties of a second-order quantum phase transition that arises in the IBM1 from a vibrational system with U(5) symmetry to a gamma-unstable deformed system with O(6) symmetry. This phase transition can be modeled by the one-parameter IBM1 Hamiltonian

FIG. 10. Evolution of the pairon positions as a function of the scaled strength parameter x for a model with ten s and d bosons subject to a Hamiltonian with linear single-boson energies and a repulsive boson pairing interaction. The circles at $x=0$ denote the positions of the s and d orbitons.

$$H = \hat{n}_d + \frac{x}{2} P^\dagger P, \qquad (59)$$

where $\hat{n}_d = \Sigma_\mu d_\mu^\dagger d_\mu$, $P^\dagger = s^\dagger s^\dagger - \Sigma_\mu (-1)^\mu d_\mu^\dagger d_{-\mu}^\dagger$, $s^\dagger$ creates a boson with angular momentum $L=0$, $d_\mu^\dagger$ creates a boson with angular momentum $L=2$ and z projection μ ($-2 \leq \mu \leq 2$), and x is the ratio of the pairing strength g to the single-particle splitting $\varepsilon_d - \varepsilon_s$. The parameter x can be varied from $x=0$ [the U(5) limit] to $x=\infty$ [the O(6) limit]. Equation (59) is an example of an exactly solvable repulsive pairing Hamiltonian, and the second-order nature of the phase transition it describes has been recently attributed to quantum integrability (Arias *et al.*, 2003).

The electrostatic problem that corresponds to this quantum boson model consists of two orbitons with positive charges $q_s = 1/4$ and $q_d = 5/4$ (see Sec. III). Both the s and d orbitons are located on the real axis, with the s located at position 0.0 and the d at position 2.0. There are M pairons with positive unit charge that interact with the orbitons and with one another and that feel an external electric field pointing downwards with strength $1/x$. In the ground-state configuration, the pairons are constrained to move between the two orbitons.

Figure 10 shows the pairon positions for a system of ten bosons as a function of the control parameter x. For x close to 0, corresponding to weak repulsive pairing, there is a very strong electric field, which compresses the pairons very close to the s orbiton. As x increases, the electric field decreases and the Coulomb repulsion among all the charges begins to counteract the effects of the external field. As a consequence, the pairons gradually expand along the energy interval between the s and the d orbitons. The phase transition between the vibrational U(5) system and the gamma-unstable O(6) system, clearly depicted in the classical electrostatic problem, arises when the Coulomb repulsion and the external electric field balance one another. Prior to the phase

transition, the quantum system is primarily an s boson condensate, with perturbative contributions from d bosons. Following the phase transition, it is a fragmented condensate mixing the s and d bosons.

A similar analysis by Dukelsky and Pittel (2001) has also been carried out for a system with many even angular momentum boson degrees of freedom, not just the s and d. The purpose of that analysis was to better understand why the IBM1, with just s and d bosons, works so well in describing the collective properties of nuclei. Recognizing that bosons in this model are an ideal representation of the lowest fermion pairs of identical nucleons and that there are not just 0^+ and 2^+ pairs, a natural question to ask is: Why can we ignore the higher-angular-momentum pairs/bosons when dealing with nuclear collective properties? Part of the answer is contained in the dominant quadrupole-quadrupole neutron-proton interaction, which is known to favor the lowest 0^+ and 2^+ pair degrees of freedom. Dukelsky and Pittel (2001) suggested another mechanism, based on an analysis of a generalized boson model containing all even angular momenta up to some maximum and interacting via a repulsive boson pairing interaction. The latter is a means of simulating the repulsive interaction between bosons that arises due to the Pauli principle between the fermion (nucleon) constituents of which they are comprised. Using the Richardson solution of this model, they showed that a repulsive boson pairing interaction can only correlate two boson degrees of freedom, and that these should be the lowest two, the s and the d. More recently, this result has been interpreted by means of electrostatic mapping (Pittel and Dukelsky, 2003). Even in the presence of many boson degrees of freedom and thus many orbitons, the collective pairons are always confined to lie between the lowest two, i.e., between the s and the d.

D. Application to a boson system confined by a harmonic-oscillator trap

We now consider the problem of a set of bosons confined to a harmonic-oscillator trap and subject to a boson pairing interaction. We claim that such a Hamiltonian cannot realistically describe the physics of a confined boson system, for the following reason. Looking back at the commutators of the pair operators $A_l^\dagger$ given in Eq. (2), we see that they are normalized to the square root of the degeneracy Ω_l of the level l. Thus the pairing-model Hamiltonian of Eq. (4) has a pairing matrix element proportional to $\sqrt{\Omega_l \Omega_{l'}}$. In a three-dimensional harmonic confining potential, these degeneracies are in turn proportional to l^2, where l plays the role of the principal quantum number and the summation in the pair operators of Eq. (1) now includes both the orbital and the magnetic quantum numbers. On the other hand, the single-boson energies ε_l for such a confining potential are linear in l. Thus a boson pairing interaction in the presence of a confining oscillator trap would have the net effect of scattering boson pairs to
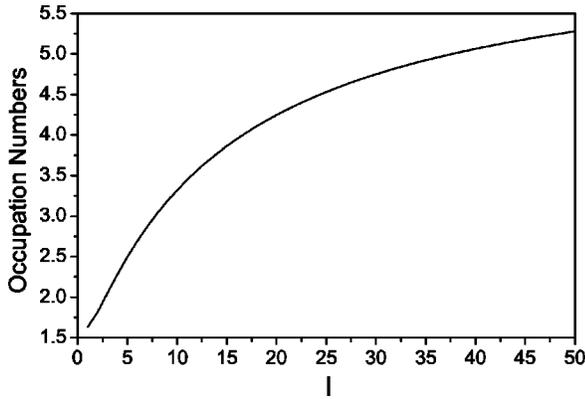
FIG. 11. Occupation numbers for 1000 bosons confined in 50 harmonic-oscillator shells and interacting via a pure pairing interaction with strength $g=-0.0025$. The occupation of the $l=0$ state is off scale and thus not shown.

FIG. 12. Occupation numbers for 1000 bosons confined in 50 harmonic-oscillator shells and interacting via a renormalized pairing interaction [see Eq. (62)] with $g=-1.0$.

high-lying levels with greater probability than to low-lying levels, producing unphysical occupation numbers.

To test this conjecture numerically, we have solved the Richardson equations [Eq. (34)] for a system of 1000 bosons ($M=500$) trapped in a three-dimensional harmonic oscillator [$\Omega_l=(l+1)(l+2)/2$ and $\varepsilon_l=\hbar\omega(l+3/2)$] with a cutoff at $101/2\hbar\omega$ ($L=50$ single boson levels). Following Richardson (1968), the occupation numbers can be calculated as

$$\langle\hat{n}_l\rangle = \left\langle\frac{\partial H_p}{\partial\varepsilon_l}\right\rangle = \sum_p \frac{\partial E_p}{\partial\varepsilon_l}. \qquad (60)$$

From Eqs. (4) and (34), a set of M coupled nonlinear equations in terms of M new unknowns are obtained, which when solved give the L occupation numbers. For details of the derivation, see Richardson (1968).

In Fig. 11, we show the occupation numbers versus the single-boson energies in units of $\hbar\omega$ for a pairing strength of $g=-0.0025$. We have excluded the occupation of the $l=0$ condensed boson state from the figure, since it lies outside the scale of the figure. The overall depletion is 0.21, which gives an occupation of the $l=0$ state of $n_0=790$ bosons. The figure clearly shows that the depletion is unphysically dominated by the high-lying (i.e., high-l) levels, due to the nature of the pair-coupling matrix elements discussed above.

We can use the freedom we have in choosing the parameters η_l entering in the definition of the R operators to obtain a more physical exactly solvable model. In order to cancel the unphysical dependence of the pair-coupling matrix elements on the degeneracies, we choose the η_l parameters so that $\eta_l=(\varepsilon_l)^3$. Then the new Hamiltonian, which is given by the associated linear combination of R_l operators, will be

$$H = 2\sum_l \varepsilon_l R_l = C + \sum_l \bar{\varepsilon}_l n_l + \sum_{l\neq l'} V_{ll'}[A_l^\dagger A_{l'} - n_l n_{l'}],$$

$$(61)$$

where

$$C = \frac{1}{2}\sum_l \varepsilon_l\Omega_l - \frac{1}{4}\sum_{l\neq l'} V_{ll'}\Omega_l\Omega_{l'},$$

$$\bar{\varepsilon}_l = \varepsilon_l - \sum_{l'(\neq l)} V_{ll'}\Omega_{l'},$$

$$V_{ll'} = \frac{g}{2}\frac{1}{\varepsilon_l^2 + \varepsilon_{l'}^2 + \varepsilon_l\varepsilon_{l'}}. \qquad (62)$$

Taking into account that ε_l is proportional to l, the two-body matrix elements in Eq. (62) cancel the dependence on the degeneracies in the effective pair-coupling matrix elements. Thus the above Hamiltonian should be more appropriate when modeling a harmonically confined boson system with a pairinglike interaction.

The interaction in Eq. (62) has the nice feature that its two-body matrix elements decrease with the number of shells, as one would expect in general. It has the particular property that the interactions of the pair and density fluctuations are strictly the same but opposite in sign. The energy eigenvalues of this Hamiltonian can be obtained from the eigenvalues r_l of the associated R_l operators as $E=2\Sigma_l\varepsilon_l r_l$, with the end result being

$$E = \frac{1}{2}\sum_l \varepsilon_l\Omega_l - \frac{1}{4}\sum_{l\neq l'} V_{ll'}\Omega_l\Omega_{l'} - 2g\sum_{lp}\frac{\varepsilon_l\Omega_l}{2\varepsilon_l^3 - E_p}. \quad (63)$$

Note that the first two terms in the energy eigenvalues of Eq. (63) exactly cancel the constant term C in Eq. (61).

We have solved the Richardson equations for the Hamiltonian of Eq. (62), i.e., with $\eta_l=(\varepsilon_l)^3$, for the same system considered above, namely, $M=500$ and $L=50$. In Fig. 12, we show the occupation numbers for $g=-1.0$, for which the overall depletion factor is 0.245. They display a reasonable physical pattern, with the occupancies decreasing monotonically with increasing single-boson energy. A comparison between the exact results and such approximations as Hartree-Fock-Bogolyubov theory or its number-conserving variants will be the subject of future work.
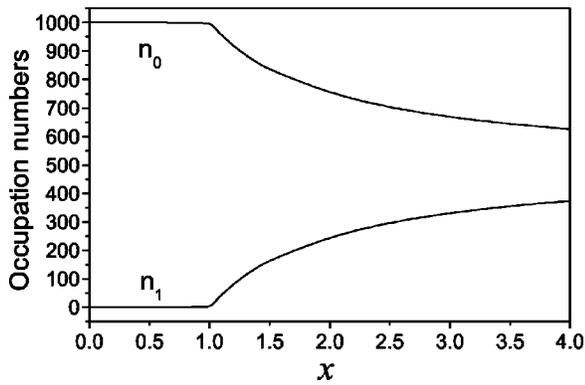
FIG. 13. Occupation numbers n_0 and n_1 for 1000 bosons confined to 50 harmonic-oscillator shells and interacting via a repulsive renormalized pairing interaction as a function of the scaled strength parameter x.

When the same modified form for the Hamiltonian, but with repulsive pairing, was considered, a highly unexpected feature was found (Dukelsky and Schuck, 2001). Figure 13 shows the occupation numbers of the first and second levels versus the scaled pairing interaction $x = 2Mg/\hbar\omega$ for the same system as above ($M = 500$, $L = 50$). At the critical value of the scaled interaction, $x_c = 1$, the normal ground-state boson condensate suddenly changes into a new phase in which the bosons occupy the $l = 0$ and the $l = 1$ levels, with the occupation of all other levels negligible.

This new phase is characterized in the large-N limit by having two macroscopically occupied states, thus representing a fragmented condensate. It is commonly accepted since the work of Nozières and Saint James (1982) that for confined systems fragmentation cannot occur in systems of scalar bosons with repulsive interactions. This might be the first example of fragmentation in a confined boson system.

VII. SUMMARY AND OUTLOOK

In this Colloquium, we have reviewed recent efforts to develop exactly solvable models of the Richardson-Gaudin type and have discussed how these models have been used to provide valuable insight into the physics of systems with strong pair correlations. We began with a brief review of Richardson's original treatment of the pairing model and Gaudin's related treatment of the Gaudin magnet and then showed how they could be generalized to several classes of exactly solvable models that still preserve a pairinglike structure.

A very attractive feature of these models is that one can establish an exact analogy between the associated quantum many-body problem and the classical physics of a two-dimensional electrostatic system. This feature, which was originally appreciated by both Richardson and Gaudin, has now been generalized to all such exactly solvable models.

The solution to a classical problem is typically amenable to simple geometrical interpretation, which can

then be used to give an alternative perspective on the quantum model from which it derives. This has been used in several examples we have discussed, for both boson and fermion systems. It provides a new perspective on how superconductivity arises in fermion models and also an interesting new perspective on a second-order quantum phase transition that arises in the nuclear interacting boson model.

Another important outcome of the classical electrostatic analogy is that it facilitates a treatment of these models in the thermodynamic limit. Not surprisingly, it shows that BCS theory is indeed the correct large-N limit of the fermion pairing model with attractive interactions.

The generalization of Richardson and Gaudin's models was first discussed in the context of the physics of small metallic grains, as a means of obtaining exact solutions to the BCS Hamiltonian appropriate to such systems in cases where numerical diagonalization was out of the question. As discussed in some detail in this Colloquium, the existence of a method of exact solution for this model provides important insight into the detailed physics present when the size of the system gets small enough so that superconductivity disappears. Neither BCS theory nor number-projected BCS theory can capture the physics of the phase transition acceptably.

The new families of exactly solvable models that we have discussed are based on the algebras SU(2) (for fermion systems) or SU(1,1) (for boson systems). These two algebras have a pseudospin representation in terms of fermion pairs or boson pairs, respectively. All applications to date and all that we have therefore discussed are based on these representations of the associated algebras. At the same time, the SU(2) group has other possible representations in terms of spin operators or two-level atoms which have not yet been exploited.

Perhaps, the most important feature of the exactly solvable Richardson-Gaudin models is the enormous freedom within an integrable family. For a given set of L single-particle levels (or orbits), we can define an exactly solvable Hamiltonian in terms of $L+1$ η_i and g parameters that enter in the definition of the associated quantum invariants [Eqs. (29) and (30)], and an additional set of L parameters ε_i that define a Hamiltonian as a linear combination of the quantum invariants. The models therefore contain $2L+1$ free parameters, which allows enormous flexibility in constructing a general pairinglike interaction tailored to the physical problem of interest (Dukelsky *et al.*, 2003). In contrast, most other exactly solvable models have either no free parameters (the Heisenberg model), one free parameter (the *XXZ* model, the Hubbard model, or the Elliott model), or just a few free parameters (the three dynamical symmetry limits of the nuclear interacting boson model). We reported here one particularly interesting use of this flexibility, namely, to model the physics of bosons confined to a harmonic trap. A pure pairing interaction has the anomalous feature that it scatters pairs of bosons preferentially to high-energy states. By exploiting the flexibility of the generalized Richardson-Gaudin models, it

was possible to find a more physically meaningful Hamiltonian for such systems, which nevertheless was still exactly solvable. Analysis of this new model led to a suggestion that confined boson systems can exist in a fragmented state, contrary to prior expectations.

All the applications discussed in this Colloquium made use of generalized Richardson-Gaudin models of the so-called rational class. Other interesting applications within this class of models should certainly be sought.

A potentially interesting example concerns the properties of the pairing phase transition in finite Fermi systems at finite temperature. There has already been important work reported on this topic [see, for example, Dean and Hjorth-Jensen (2003) and references therein]. As noted earlier, the exact solution of the pairing model can be derived from the algebraic Bethe ansatz. It is natural therefore to study the thermodynamic Bethe ansatz, which provides the exact finite-temperature description of short-range 1D integrable models, to see whether it could be extended for application to integrable pairing models. If so, this would allow for an exact treatment of the finite-temperature properties of such systems as nuclei, ultrasmall superconducting grains, and degenerate Fermi gases.

Another important topic that has recently received attention (Dean and Hjorth-Jensen, 2003) is the study of the low-energy properties of quantum many-body systems with random interactions and in particular with random pairing interactions. Though random pairing interactions in general have chaotic properties, there is an important subset of integrable pairing Hamiltonians that have a large number of free parameters which can be chosen randomly. Some of the physical consequences of randomly chosen pairing interactions in the general chaotic regime and within the integrable subset of pairing models have been reported recently by Volya *et al.* (2002) and Relaño *et al.* (2004).

We also expect interesting applications to ensue for the trigonometric and hyperbolic models. As one example, the trigonometric model was used by Gaudin (1976) to derive the limit of an exactly solvable model of the interaction of a two-level atomic system with an external oscillator field. This kind of model could lead to a generalization of the celebrated Jaynes-Cummings model. Using techniques similar to the algebraic Bethe ansatz derivation of the Richardson model, exactly solvable models for boson atomic-molecule systems and two coupled Bose-Einstein condensates have recently been found (Links *et al.*, 2003). Based on these arguments, we believe that Richardson-Gaudin models could have a promising future in quantum optics and in the study of dilute Fermi and Bose gases (Dukelsky *et al.*, 2004).

Another area of great interest is the generalization of Richardson-Gaudin models based on the SU(2) or SU(1,1) algebras to larger algebras. Some work has already been reported along these lines (Asorey *et al.*, 2002). A complete solution for models with O(5) or SU(4) symmetries could lead to interesting applications for nuclear systems with $N \approx Z$, where it is important to include explicitly the isospin degree of freedom. It could also provide useful insight into the properties of high-T_c superconductors (Zhang, 1997; Wu *et al.*, 2002). Though in previous works Richardson (1966b, 1967) proposed an exact solution for pairing Hamiltonians with these two group symmetries, recent work by Pan and Draayer (2002) indicates that his solution is invalid for systems with more than two pairs. Moreover, Links *et al.* (2002) and Guan *et al.* (2002) have found different solutions for the same problems. More work is clearly required along these lines.

In closing, the use of exactly solvable Richardson-Gaudin models has already provided significant new and important insight into the properties of many diverse quantum systems, ranging from atomic nuclei to electronic systems in condensed matter. We are optimistic that many more exciting applications are still to come.

REFERENCES

Amico, L., A. Di Lorenzo, A. Mastellone, A. Osterloh, and R. Raimondi, 2002, Ann. Phys. (N.Y.) **299**, 228.

Amico, L., A. Di Lorenzo, and A. Osterloh, 2001, Phys. Rev. Lett. **86**, 5759.

Amico, L., G. Falci, and R. Fazio, 2001, J. Phys. A **34**, 6425.

Anderson, P. W., 1958, Phys. Rev. **112**, 1900.

Anderson, P. W., 1959, J. Phys. Chem. Solids **11**, 28.

Arias, J. E., J. Dukelsky, and J. E. García-Ramos, 2003, Phys. Rev. Lett. **91**, 162502.

Arrachea, L., and M. J. Rozenberg, 2001, Phys. Rev. Lett. **86**, 5172, and private communication.

Asorey, M., F. Falceto, and G. Sierra, 2002, Nucl. Phys. B **622**, 593.

Baldo, M., J. Cugnon, A. Lejeune, and U. Lombardo, 1990, Nucl. Phys. A **515**, 409.

Bang, J., and J. Krumlimde, 1970, Nucl. Phys. A **141**, 18.

Bardeen, J., L. N. Cooper, and J. R. Schrieffer, 1957, Phys. Rev. **108**, 1175.

Berger, S. D., and B. I. Halperin, 1998, Phys. Rev. B **58**, 5213.

Bethe, H. A., 1931, Z. Phys. **71**, 265.

Braun, F., and J. von Delft, 1998, Phys. Rev. Lett. **81**, 4712.

Calogero, F., 1962, J. Math. Phys. **10**, 2191.

Cambiaggio, M. C., A. M. F. Rivas, and M. Saraceno, 1997, Nucl. Phys. A **624**, 157.

Dean, D. J., and M. Hjorth-Jensen, 2003, Rev. Mod. Phys. **75**, 607.

Dietrich, K., H. J. Mang, and J. H. Pradal, 1964, Phys. Rev. **135**, B22.

Dukelsky, J., G. G. Dussal, C. Esebbag, and S. Pittel, 2004, Phys. Rev. Lett. (to be published).

Dukelsky, J., C. Esebbag, and S. Pittel, 2002, Phys. Rev. Lett. **88**, 062501.

Dukelsky, J., C. Esebbag, and P. Schuck, 2001, Phys. Rev. Lett. **87**, 066403.

Dukelsky, J., and S. Pittel, 2001, Phys. Rev. Lett. **86**, 4791.

Dukelsky, J., J. M. Román, and G. Sierra, 2003, Phys. Rev. Lett. **90**, 249803.

Dukelsky, J., and P. Schuck, 2001, Phys. Rev. Lett. **86**, 4207.

Dukelsky, J., and G. Sierra, 1999, Phys. Rev. Lett. **83**, 172.

Dukelsky, J., and G. Sierra, 2000, Phys. Rev. B **61**, 12302.

Elliott, J. P., 1958a, Proc. R. Soc. London, Ser. A **242**, 128.

Elliott, J. P., 1958b, Proc. R. Soc. London, Ser. A **242**, 562.

Gaudin, M., 1976, J. Phys. (Paris) **37**, 1087.

Gaudin, M., 1995, *États Propres et Valeurs Propres de l'Hamiltonien d'Appariement* (Les Éditions de Physique, France).

Gould, M. D., Y.-Z. Zhang, and S.-Y. Zhao, 2002, Nucl. Phys. B **630**, 492.

Guan, X.-W., A. Foerster, J. Links, and H.-Q. Zhou, 2002, Nucl. Phys. B **642**, 501.

Ha, Z. N. C., 1996, *Quantum Many-Body Systems in One Dimension* (World Scientific, Singapore).

Haldane, F. D. M., 1981, J. Phys. C **14**, 2585.

Haldane, F. D. M., 1988, Phys. Rev. Lett. **60**, 635.

Hasegawa, M., and S. Tasaki, 1987, Phys. Rev. C **35**, 1508.

Hasegawa, M., and S. Tasaki, 1993, Phys. Rev. C **47**, 188.

Heiselberg, H., 2003, Phys. Rev. A **68**, 053616.

Heritier, M., 2001, Nature (London) **414**, 31.

Iachello, F., and A. Arima, 1980, *The Interacting Boson Model* (Cambridge University, Cambridge, England).

Links, J., H.-Q. Zhou, M. D. Gould, and R. H. McKenzie, 2002, J. Phys. A **35**, 6459.

Links, J., H.-Q. Zhou, R. H. McKenzie, and M. D. Gould, 2003, J. Phys. A **36**, R63.

Luttinger, J. M., 1963, J. Math. Phys. **15**, 609.

Mastellone, A., G. Falci, and R. Fazio, 1998, Phys. Rev. Lett. **80**, 4542.

Matveev, K. A., and A. I. Larkin, 1997, Phys. Rev. Lett. **78**, 3749.

Nozières, P., and D. Saint James, 1982, J. Phys. (Paris) **43**, 1133.

Pan, F., and J. P. Draayer, 2002, Phys. Rev. C **66**, 044314.

Pittel, S., and J. Dukelsky, 2003, nucl-th/0309020.

Ralph, D. C., C. T. Black, and M. Tinkham, 1997, Phys. Rev. Lett. **78**, 4087.

Relano, A., J. Dukelsky, J. M. G. Gomez, and J. Retamosa, 2004, Phys. Rev. E (to be published).

Richardson, R. W., 1963a, Phys. Lett. **3**, 277.

Richardson, R. W., 1963b, Phys. Lett. **5**, 82.

Richardson, R. W., 1965, J. Math. Phys. **6**, 1034.

Richardson, R. W., 1966a, Phys. Rev. **141**, 949.

Richardson, R. W., 1966b, Phys. Rev. **144**, 874.

Richardson, R. W., 1967, Phys. Rev. **159**, 792.

Richardson, R. W., 1968, J. Math. Phys. **9**, 1327.

Richardson, R. W., 1977, J. Math. Phys. **18**, 1802.

Richardson, R. W., and N. Sherman, 1964, Nucl. Phys. **52**, 221.

Roman, J. M., G. Sierra, and J. Dukelsky, 2002, Nucl. Phys. B **634**, 483.

Roman, J. M., G. Sierra, and J. Dukelsky, 2003, Phys. Rev. B **67**, 064510.

Rombouts, S., D. Van Neck, and J. Dukelsky, 2003, Phys. Rev. B (to be published).

Schechter, M., Y. Imry, Y. Levinson, and J. von Delft, 2001, Phys. Rev. B **63**, 214518.

Shastry, B. S., 1988, Phys. Rev. Lett. **60**, 639.

Shastry, B. S., and A. Dhar, 2001, J. Phys. A **34**, 6197.

Sierra, G., 2000, Nucl. Phys. B **572**, 517.

Sierra, G., 2002, in *Statistical Field Theories*, edited by A. Cappelli and G. Mussardo, NATO Sciences Series, Vol. 73 (Kluwer Academic, London), pp. 317–328.

Sierra, G., J. Dukelsky, G. G. Dussel, J. von Delft, and F. Braun, 2000, Phys. Rev. B **61**, R11 890.

Sigrist, M., and K. Ueda, 1991, Rev. Mod. Phys. **63**, 239.

Smith, R. A., and V. Ambegaokar, 1996, Phys. Rev. Lett. **77**, 4962.

Sutherland, B., 1971, J. Math. Phys. **12**, 246.

Tomonaga, S., 1950, Prog. Theor. Phys. **5**, 544.

Volya, A., V. Zelevinsky, and B. A. Brown, 2002, Phys. Rev. C **65**, 054312.

von Delft, J., D. S. Golubev, W. Tichy, and A. D. Zaikin, 1996, Phys. Rev. Lett. **77**, 3189.

von Delft, J., and R. Poghossian, 2002, Phys. Rev. B **66**, 134502.

von Delft, J., and D. C. Ralph, 2001, Phys. Rep. **345**, 61.

Wu, L.-A., M. W. Guidry, Y. Sun, and C.-L. Wu, 2002, Phys. Rev. B **67**, 014515.

Yuzbashyan, E. A., A. A. Baytin, and B. L. Altshuler, 2003, Phys. Rev. B **68**, 214509.

Zhang, S.-C., 1997, Science **275**, 1089.

Zhou, H.-Q., J. Links, R. H. McKenzie, and M. D. Gould, 2002, Phys. Rev. B **65**, 060502.